Climate and Glacier Variability in Western North America

L. A. RASMUSSEN AND H. CONWAY

Department of Earth and Space Sciences, University of Washington, Seattle, Washington

(Manuscript received 16 June 2003, in final form 17 November 2003)

ABSTRACT

A simple model using once-daily upper-air values in the NCEP–NCAR reanalysis database estimates seasonal mass balance at two glaciers in southern Alaska, one in western Canada, and one in Washington substantially better than any of several seasonally averaged, large-scale climate indices commonly used. Whereas sea level pressure and sea surface temperature in the Pacific exert a strong influence on the climate in the region, temperature and moisture flux at 850 mb have a more direct effect on mass balance processes—accumulation and ablation—because their temporal variability better matches that of those processes. The 40-yr record of 850-mb temperature shows winter warming after 1976 and summer warming after 1988 throughout the region; mass balance records reflect the summer warming at all four glaciers but winter warming only at the southern two. The only pronounced long-term change in the moisture regime is a decrease of precipitation in the south and an increase in the north. Interannual variations in the location of the moisture flux, however, apparently account for the strong negative correlation between the Alaska glaciers and the other two.

1. Introduction

This study investigates the relation between seasonal mass balance components and meteorological conditions in the region of the large concentration of ice in southern Alaska (Fig. 1). Because of the paucity of observations of seasonal mass balance in Alaska, two glaciers farther south are included. Place Glacier in western British Columbia and especially South Cascade Glacier in Washington have had good long-term observation programs. A principal objective is comparing estimation of mass balance from daily variations of upper-air conditions with correlations between mass balance and seasonally averaged large-scale climate indices. Another is demonstrating trends over the past several decades in mass balance and in upper-air conditions.

There has been increasing attention recently to the contribution to global sea level rise of thinning of the 90 000 km^2 of glaciers, principally in southern Alaska and secondarily in adjacent Canada (Meier and Dyurgerov 2002). Arendt et al. (2002) compared the annual thinning rate of 27 glaciers there, which they profiled with airborne laser altimetry about 1995 and about 5 years later, with the thinning rate for about 40 years before that period. Most of the great increase in thinning they reported was due to just two tidewater glaciers—the drastic retreat and thinning of Columbia Glacier beginning about 1980 and the 1993–95 surge of Bering Glacier—but the other 25 glaciers had an average increase of annual thinning rate of about 50% from the earlier period to the later one.

Although the drastic retreat of tidewater glaciers may be caused by the cumulative effect of decades or centuries of diminished mass balance, it does not provide information on the interannual variations of mass balance or of its relation to climate. Both glacier surges, which are not well understood, and retreat of tidewater glaciers can lead to marked thinning, but both of these processes are influenced by the topography of the bed on which they lie, as well as on the gain or loss of mass due to mass balance processes. The instrumental record of climate in Alaska is very sparse before about 1950 and is nearly nonexistent before 1900.

a. Mass balance components

The most commonly reported mass balance information for a glacier is the interannual variation of mass change, which is expressed as the thickness change averaged over the entire glacier area and is given in water-equivalent meters. Two different time bases are customarily used (Mayo et al. 1972): 1) the fixed-date method, usually from 1 October to 1 October in the Northern Hemisphere, is termed the *annual balance,* and 2) the change from the time of minimum mass at the end of one summer to the time of minimum mass at the end of the following summer is termed the *net balance.* The two methods give comparable results in northern temperate climates because the date of minimum mass is

Corresponding author address: Al Rasmussen, Department of Earth and Space Sciences, University of Washington, Box 351310, Seattle, WA 98195-1310.
E-mail: LAR@geophys.washington.edu

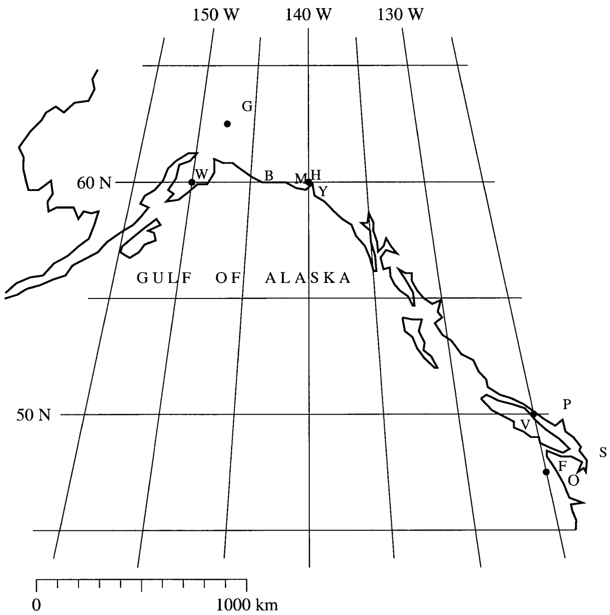

FIG. 1. Western North America. NCEP–NCAR reanalysis grid points are at intersections of lines and also at intermediate latitudes and longitudes, that is, every 2.5°. Solid circles are grid points used in estimating mass balance or precipitation (Table 3). Glaciers are Bering B, Gulkana G, Hubbard H, Malaspina M, Place P, South Cascade S, and Wolverine W. Precipitation stations are Forks F and Yakutat Y. Olympic Peninsula is O, and Vancouver Island is V.

usually near 1 October and because the rate of thickness change then is small compared with the rate in either summer or winter. Reported values often do not distinguish between the two time bases of interannual variations. We refer to interannual values generically as net balance b_n.

Seasonal components are winter balance b_w accounting for the gain of mass from the beginning of the balance year until its maximum, usually late the following spring, and the summer balance b_s accounting for the loss of mass after then until the end of the balance year. Winter balance is the resultant difference between a large amount of accumulation and a small amount of ablation, whereas summer balance is the resultant difference between a large amount of ablation and a small amount of accumulation. The three components are related simply by

$$b_n = b_w + b_s, \tag{1}$$

with b_s defined to be a negative quantity. All three components are identified by the calendar year in which the balance year ends.

Thickness change of glaciers in this region has been sparsely sampled both temporally and spatially. At South Cascade Glacier, for instance, winter accumulation of snow is probed at many sites on a glacier usually once in spring, with its density either estimated or measured at one site, and interannual changes are measured by a few stakes drilled into the ice (Krimmel 2000).

TABLE 1. Average mass balance (m w.e.) over the period given in Fig. 2.

Glacier	b_w	b_s	b_n
Wolverine	2.37	−2.69	−0.32
Gulkana	1.07	−1.54	−0.47
Place	1.75	−2.56	−0.81
S. Cascade	2.72	−3.18	−0.47

Spring visits may occur weeks before or after the date of maximum mass, as may autumn visits relative to the date of minimum mass. As a result, reported values are accurate to within only a few tenths of a meter (Krimmel 2000, Table 16).

b. *The glaciers*

The U. S. Geological Survey initiated research programs on South Cascade in Washington in 1959 and on Wolverine and Gulkana in southern Alaska in 1966 (Meier et al. 1971). Mass balance measurements were begun at Place Glacier in western Canada in 1965 by the National Glaciology Programme of the Geological Survey of Canada (Moore and Demuth 2001). Averages over the complete period of record are given in Table 1 for each of the three balance components. Wolverine, Place, and South Cascade are all in marine climates, whereas Gulkana's is continental; all of them terminate on land.

Wolverine Glacier is a 17.6 km^2 south-facing glacier on the Kenai Peninsula. The Gulf of Alaska is about 50 km to the east. Although most of the glacier is between 1000 and 1700 m, a narrow tongue extends down to 400 m.

Gulkana Glacier is a 19.3 km^2 glacier in the eastern part of the Alaska Range, ranging in altitude between 1160 and 2160 m. It is south facing on the south slope of the range. Exposure to moist air from the Gulf of Alaska, about 300 km to the south, is impeded by high mountains near the coast.

Place Glacier is a 3.4 km^2 north-facing glacier on the lee side of the Cascade Range of British Columbia about 250 km from the Pacific Ocean. It ranges in altitude between 1850 and 2600 m. Its exposure to moist air from the Pacific is also impeded by mountains, both on the mainland and on Vancouver Island.

South Cascade Glacier is a 2.0 km^2 north-facing glacier on the crest of the north Cascades in Washington, 250 km from the Pacific Ocean. It ranges in altitude between 1630 and 2130 m. Its exposure to air from the Pacific from the west-southwest is impeded by the Olympic Mountains but not to air from the west or southwest. The glacier is not in equilibrium with the recent climate, having retreated and thinned substantially (Krimmel 2002) over the past 150 years. Moreover, if climate conditions of the past 15 years continue, it will shrink to about a quarter of its present size (Rasmussen and Conway 2001).

TABLE 2. Mass balance correlations (% r) over periods given in Fig. 2. Correlations significant at the 95% level are in boldface.

	b_w			b_s			b_n		
Glacier	G	P	S	G	P	S	G	P	S
Wolverine (W)	−4	**−37**	**−50**	**+49**	+22	−14	**+51**	−18	**−49**
Gulkana (G)		−26	−28		+1	−16		−20	−28
Place (P)			**+57**			**+58**			**+63**
S. Cascade (S)									

c. Glacier covariability

Walters and Meier (1989) calculated correlations of net balance b_n over 1966–85 between all pairs of the six glaciers they studied. Hodge et al. (1998) extended the calculations to 1995; they also included the two seasonal balances b_w and b_s but considered only South Cascade, Wolverine, and Gulkana. Both those analyses noted the positive correlation between the two Alaska glaciers, except for b_w, and their negative correlation with South Cascade, although the latter work noted deterioration of those negative correlations in recent years.

Those three-glacier, three-balance results persist in the calculations extended here through 1999 (Table 2). Most prominent are the positive correlations between Place and South Cascade for all three components as well as between Wolverine and Gulkana for b_s and b_n but not for b_w. The poor correlation between Wolverine and Gulkana was interpreted by Hodge et al. (1998) as being due to Wolverine being in a marine climate, Gulkana in a continental one. Correlations between the Alaska glaciers and the southern glaciers are moderately negative for b_w and b_n and are nearly nonexistent for b_s.

Time series of each component are shown in Fig. 2 for all four glaciers. Two-stage piecewise-constant functions (see section 5: Trends) are arbitrarily adopted for each series, although for Wolverine b_w a three-stage function may be more appropriate, as noted by Hodge et al. (1998, Table 1). Only at Place and South Cascade is there a pronounced decrease in b_w, in the 1970s, but

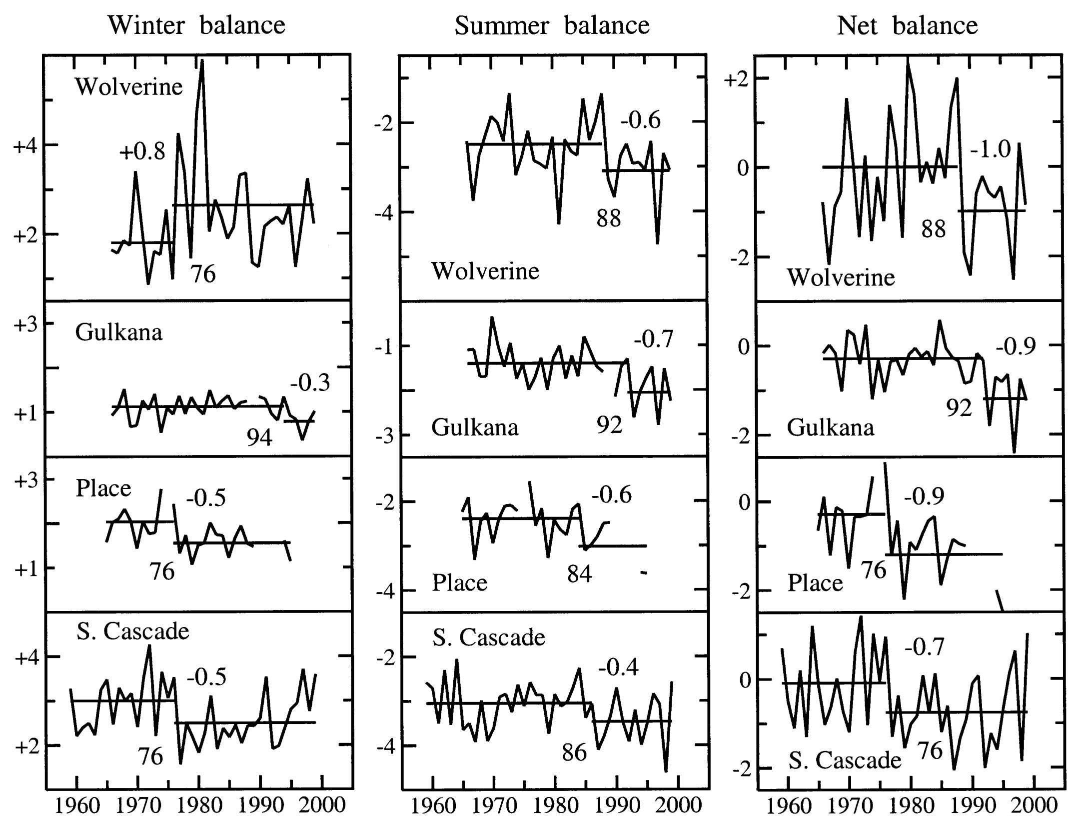

FIG. 2. Time series of balance components: 1959–99 except that Wolverine and Gulkana began 1966, Gulkana lacks seasonal balances for 1989, and Place reported only 1965–74, 1976–89, and 1994–95. Annual resolution: The unsigned number indicates last year of the first stage of the best-fitting piecewise-constant function, and the signed number the difference between the mean values of the two stages. All plots are at the same vertical scale in meters.

there is for b_s at all four glaciers 1984–92. Strong negative discontinuities are present in b_n for all four glaciers. Although b_n has opposite sign in the north and the south in most individual years, the long-term trend is negative in both.

d. Previous work

Covariability of mass balance of glaciers in the region stretching from southern Alaska to western Washington (Fig. 1) has been the subject of recent studies. Walters and Meier (1989) used empirical orthogonal function (EOF) analysis to investigate relations between net balance values at the four glaciers, as well as at two others in western Canada, over 1966–85. They found a pronounced negative correlation between mass balance at the Alaska glaciers and the two to the south. They attributed this to the effect of the position of the Aleutian low pressure system in steering storms toward either the north or the south.

McCabe and Fountain (1995) found negative correlation between the height of the 700-mb level over western Canada and winter balance at Place and South Cascade. They interpreted their result as another indication of the location of storm tracks in the region. High pressure over western Canada tends to steer storms to the north, low pressure to the south.

Hodge et al. (1998) used records of winter balance and summer balance up to 1995 at Wolverine, Gulkana, and South Cascade. They calculated correlations between the balances and seasonal values of four different large-scale climate patterns. The Pacific–North America index (PNA) is a linear combination of the 500-mb heights at four widely spaced points over North America and the eastern Pacific. The central North Pacific index (CNP) is the average sea level pressure (SLP) over the region between 35° and 55°N, 170°E and 150°W. The Southern Oscillation index (SOI) uses the SLP difference between Darwin, Australia, and Tahiti. The two measures of sea surface temperature (SST) they used are averages over bands in the equatorial Pacific.

Bitz and Battisti (1999) compared three different November–March measures of SST with records up to 1995 of winter balance and net balance at the four glaciers, as well as at two others in western Canada. The Pacific Decadal Oscillation index (PDO) is the leading principal component of SST in the Pacific north of 20°N. The cold tongue index (CT) is SST averaged between 6°N and 6°S, 90°W and 180°. The global residual index (GR) is the principal component of the EOF of the global SST.

2. Data sources

The National Centers for Environmental Prediction–National Center for Atmospheric Research (NCEP–NCAR) reanalysis data (Kalnay et al. 1996)—which provide point values of temperature, humidity, and wind—were obtained for 1948–99 from NCAR in June 2002. The International Geophysical Year (1957/58) inspired increases in the quantity and quality of radiosonde data, and observation times changed 1 June 1957 from 0300 and 1500 UTC, to 0000 and 1200 UTC (Kistler et al. 2001; Angell 1988). Averages and trends of upper-air winds and temperatures are therefore formed here over only 1960–99. Severe biases in the humidity record prior to about 1975 occurred during the evolution of instrumentation and recording methods (Rasmussen et al. 2001, section 4) including some due to changes in sensor design and one due to inadequate shielding from solar radiation, which caused aberrantly low daytime readings. Thus, values at only 1200 UTC, which comes at night in this region, are used to lessen the effects of inhomogeneities in the historical humidity record.

Mass balance values at South Cascade Glacier for 1959–99 are given by Krimmel (2002). Values for 1986–91, however, are taken from Krimmel (2000) on the advice of R. M. Krimmel (August 2002, electronic communication). Mass balance values for the other glaciers are taken from Dyurgerov (2002).

Three other SLP indices are tested in this analysis. The North Pacific index (NP) is its average over 30°–60°N between 160°E and 140°W (Trenberth and Hurrell 1994). The Aleutian low pressure index (ALPI) is the area of the region with SLP $<$ 1000 mb (Beamish et al. 1997). The atmospheric forcing index (AFI) is a combination of ALPI, PDO, and NP (McFarlane et al. 2000).

3. Estimating mass balance from NCEP–NCAR data

a. Winter balance model

Following Rasmussen and Conway (2001), winter balance for a particular glacier is estimated from the linear relation

$$b_w^* = \alpha_w \overline{f}_w + \gamma_w, \tag{2}$$

in which α_w and γ_w are empirically determined constants and $\overline{f}_w$ is the October–May average of daily values of what is termed the snow flux

$$f = \begin{cases} U\,\mathrm{RH}, & U > 0,\ T_1 < +2^\circ\mathrm{C} \\ 0, & \text{otherwise.} \end{cases} \tag{3}$$

Here T_1 is interpolated between the 850-mb and 700-mb levels at an altitude z_1 near the glacier terminus, $0 \le \mathrm{RH} \le 1$ is the 850-mb relative humidity, and U is the component of the 850-mb wind in the empirically determined critical direction ϕ'. That is,

$$U = |\mathbf{V}_{850}|\ \cos(\phi_{850} - \phi'), \tag{4}$$

where ϕ_{850} is the wind direction and $|\mathbf{V}_{850}|$ is its speed in meters per second.

The quantity U RH, here termed the precipitation flux

TABLE 3. Glacier locations and model parameters. Direction ϕ' of 850-mb wind component is used with temperatures at z_1 and z_2 (m a.s.l.) in Eqs. (1)–(5). Yakutat is a weather station.

Glacier/Station	Location	Grid point	ϕ'	z_1	z_2
Wolverine	60.4°N, 148.9°W	60.0°N, 150.0°W	122	1100	1300
Gulkana	63.3°N, 145.4°N	62.5°N, 147.5°N	238	1400	1800
Place	50.4°N, 122.6°W	50.0°N, 125.0°W	230	1850	2100
South Cascade	48.4°N, 121.1°W	47.5°N, 125.0°W	271	1650	2000
Yakutat	59.5°N, 139.7°W	60.0°N, 140.0°W	208		

F, is used as an approximation of the divergence of the moisture flux, which corresponds directly (when the divergence is negative) to the amount of moisture removed from the air. This is done first on the assumption that, when the flow is from the sector of ϕ', the negative divergence correlates strongly with F. Second is that the empirically determined ϕ' accounts for flow generally in the topographically upslope direction. Third is the assumption that F, which strictly is a pseudoflux, is a better indicator of precipitation potential than the true moisture flux Ue, in which e is the vapor pressure or specific humidity, because precipitation is a saturation phenomenon. A fourth assumption is that the total flux in the vertical column correlates well with that at 850 mb, which is used here because it is a standard level routinely reported and archived. This level usually carries more moisture than higher levels, yet is high enough to sample free-air conditions, and its wind is strongly correlated with winds at higher levels. These assumptions are consistent with conditions Pandey et al. (1999) analyzed in California.

The critical temperature is set at $+2°C$ [Eq. (3)] because there must be a warmer layer of air below the 0°C level in which snowflakes falling from above can melt into raindrops. Rasmussen et al. (2000) found that daily observations of snow or rain August 1957 through July 1958 at Blue Glacier, 200 km toward the ocean from South Cascade, were consistent with $+2°C$ interpolated from a nearby radiosonde station. In modeling vertical gradients of mass balance in Austria, Oerlemans and Hoogendoorn (1989) used $+2°C$ as the boundary between snow and rain. The simple formulation of the winter balance model does not account for accumulation by the refreezing of rain, by avalanching, etc.

Upper-air conditions are taken from a nearby NCEP–NCAR reanalysis grid point. The grid point used and values of the model parameters ϕ' and z_1 are given for each glacier in Table 3. Temperature at the grid point is adjusted to temperature at Place or South Cascade according to the horizontal gradient obtained from the mean 850-mb field for each month (U.S. Navy 1966). For Wolverine and Gulkana, which are nearer the grid points used for them, no T adjustment is made.

b. Summer balance model

Summer balance is estimated from an extension (Rasmussen and Conway 2003) of the winter balance model with a term added to account for melt

$$b_s^* = \alpha_s \overline{f}_s + \beta_s \overline{T}_2 + \gamma_s, \tag{5}$$

in which $\overline{f}_s$ is the June–September average of daily values of the snow flux [Eq. (3)] and $\overline{T}_2$ is the June–September average of 1200 UTC temperature interpolated between the 850-mb and 700-mb levels at an altitude z_2 (Table 3) near the equilibrium line, but considering only those $T_2 > 0°C$. Coefficients α_s, β_s, γ_s are determined by linear regression.

The summer balance model does not explicitly account for radiation fluxes. Meteorological evidence from the vicinity of South Cascade, however, indicates that the fluxes correlate with $\overline{T}_2$ (Rasmussen and Conway 2003). From year to year, higher $\overline{T}_2$ is usually accompanied by more frequent clear weather with higher atmospheric transmittance and, hence, a greater amount of solar radiation reaching the glacier.

c. Model results

Net balance is estimated simply as the sum of the estimates of winter balance [Eq. (2)] and summer balance [Eq. (5)]. For all mass balance components, the root-mean-square error rmse between modeled and observed balance is comparable to observational uncertainty. Errors expressed by

$$r^2 = 1 - \left(\frac{\text{rmse}}{\sigma}\right)^2, \tag{6}$$

in which σ is the standard deviation of the quantity being estimated (b_w, b_s, or b_n), are shown in Table 4 for all three components, for all four glaciers. Also shown are r^2 obtained from the r values quoted in the studies of correlation with large-scale climate patterns (section 1b) as well as with three measures examined here (section 2). Many results are correlations with a single independent variable, in which case r is obtained, but for others such as from Eq. (5) only r^2 is, so to achieve a common basis for comparison all results in Table 4 are given as r^2.

At Place and South Cascade, which have a small altitude range, the optimum z_1 is at the glacier terminus. At Wolverine and Gulkana, however, which have a very large range, it is higher on the glacier. Presumably the crucial issue is the frequent presence of a divided precipitation regime over the glacier, with snow at high altitude and rain at low. Setting z_1 too high may detect storms that produced snow only high on the glacier,

Table 4. Correlations (% r^2) of mass balance components with large-scale climate indices. Blank cells: correlations not calculated, —: declared by authors to be ''not significant,'' and boldface: significant at the 95% level. References (Ref): 1) McCabe and Fountain (1995), 2) Hodge et al. (1998), 3) Bitz and Battisti (1999), 4) this analysis, and 5) Eqs. (1)–(5).

		Wolverine			Gulkana			Place			S. Cascade		
Index/model	Ref	b_w	b_s	b_n	b_w	b_s	b_n	b_w	b_s	b_n	b_w	b_s	b_n
700-mb height	1							**27**			**58**		
Nov–Apr SOI	2	—	—		—	—					**35**	—	
Nov–Apr SST	2	—	—		—	—					**28**	**30**	
Nov–Apr CNP	2	**49**	—		—	—					**41**	—	
Nov–Apr PNA	2	**38**	—		—	—					**37**	—	
May–Oct SOI	2		—			14						—	
May–Oct SST	2		—			14						16	
May–Oct CNP	2		—			—						17	
May–Oct PNA	2		—			—						—	
Nov–Apr GR	3	**34**		**30**	9		7	**21**		**24**	**28**		**24**
Nov–Apr PDO	3	**50**		**46**	2		7	**22**		15	**56**		**42**
Nov–Apr CT	3	5		14	1		3	4		0	**18**		**20**
Dec–Mar AFI	4	**43**	0	**33**	0	3	2	10	4	8	**36**	2	**24**
Oct–May PDO	4	**34**	0	**27**	0	0	0	**32**	**15**	**28**	**42**	**10**	**42**
Jun–Sep PDO	4	2	0	1	0	7	6	3	1	2	**18**	2	**14**
Dec–Mar ALPI	4	**41**	2	**23**	5	6	1	3	2	3	**22**	2	**16**
Nov–Mar NP	4	**26**	0	**19**	0	**27**	**20**	7	2	5	**30**	4	**23**
850-mb model	5	**64**	**55**	**79**	*42*	**65**	**63**	**63**	**53**	**62**	**76**	**71**	**79**

whereas setting z_1 too low may fail to detect storms with snow over much of the glacier above that altitude. In the case of South Cascade Glacier, results are only mildly sensitive to the value of z_1 (Rasmussen and Conway 2003).

Results are weakly sensitive to z_2 because T_2 appears linearly in Eq. (5) and because $T(z)$ is roughly linear. That is, the coefficient γ_s adjusts to accommodate alternative z_2 values by an amount roughly equal to the product of the mean vertical lapse rate dT/dz and the difference in z_2.

Moore and Demuth (2001) obtained comparable results for Place from linear regressions using winter precipitation and summer temperature at Agassiz, 150 km to the south. Over 1965–99, multiple regression with both the temperature and precipitation estimated b_n with $r^2 = 0.64$. The temperature alone estimated b_s with $r^2 = 0.51$; when b_w was used along with the temperature, b_s was estimated with $r^2 = 0.63$. They interpret the weak influence of winter temperature on b_w to be due to most winter precipitation falling as snow on this high altitude glacier even in warm winters.

Tests of the models made by interpolating between grid points instead of using the nearest grid point gave negligibly different r^2 for Wolverine or Gulkana. One reason is that spatial gradients in the reanalysis database are usually weak, and correlations between nearby grid points are strongly positive. Another is that the minimization process for finding the model parameters will adjust α_w in Eq. (2) α_s in Eq. (5) to account for different wind and humidity values. A third is that the process will adjust the optimum altitudes z_1 and z_2 to account for differences in T.

Split sample tests (Rasmussen and Conway 2001, 2003) show that the regression coefficients in Eqs. (2), (5) are highly stable. Results are not strongly sensitive to the value used for the critical direction ϕ' because of the cosine in Eq. (4); for instance, $\cos 20° = 0.94$. Nevertheless, the near orthogonality between ϕ' at Wolverine and at Gulkana (Table 3) is striking. Moreover, it is consistent with the poor correlation of winter balance between the two glaciers (Table 2). For all four glaciers ϕ' is in the direction from the nearest ocean.

The precipitation flux $F = U$ RH from Eq. (3) using direction $\phi' = 208°$ at 60°N, 140°W estimates October–May precipitation at Yakutat over 1966–99 with rmse 0.39 m ($r^2 = 0.63$). Using direction $\phi' = 228°$ at 47.5°N, 125°W it estimates it at Forks over 1960–99 with rmse 0.30 m ($r^2 = 0.66$). Whereas $\phi' = 228°$ is the optimum direction for estimating precipitation at Forks, it is 271° for estimating accumulation at South Cascade Glacier because flow from 228° is obstructed by mountains between Forks and South Cascade.

d. *Possible model refinements*

Rasmussen and Conway (2001) developed the winter balance model for South Cascade using twice-daily data from a radiosonde at a National Weather Service station near the coast. The rms error increased 10% when, as a test, the sampling was reduced to once daily. Using the 6-h resolution of the reanalysis data may improve results.

For glaciers with large altitude ranges, better results may accrue from splitting the $\overline{f}$ term [in Eq. (2) or Eq. (5)] into a term for an altitude low on the glacier and a term for one high on the glacier. Although the reanalysis database does not have fine vertical resolution, U and T_1 can be interpolated at more altitudes between the reported levels. Similarly splitting the T_2 term in

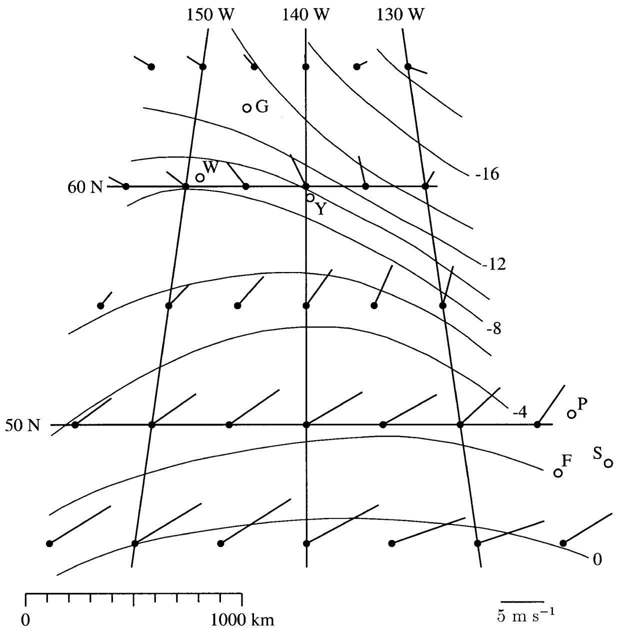

FIG. 3. Mean Jan 850-mb wind and temperature over 1966–99. The wind vector emanates from the grid point in the downstream wind direction, and its length is proportional to the speed. Isotherms are in °C, and letters indicate glaciers and weather stations (Fig. 1).

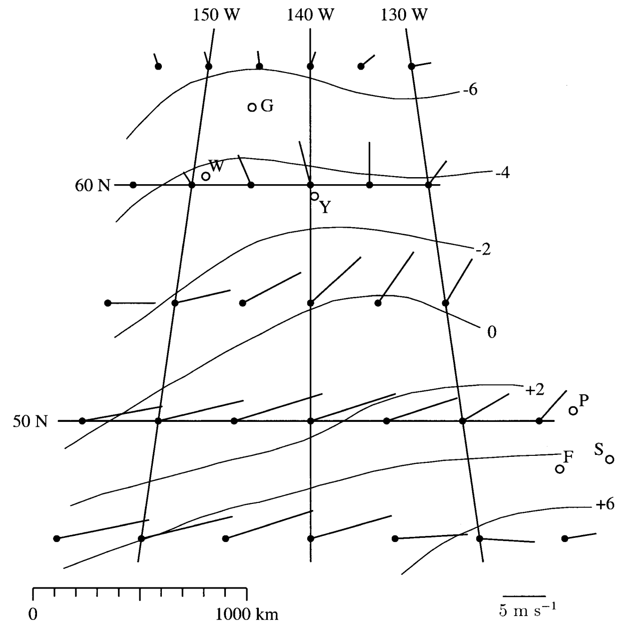

FIG. 4. As in Fig. 3 except for Oct.

Eq. (5) may improve estimates of summer balance for some glaciers. Rasmussen and Conway (2001) found, however, that for the small (500 m) altitude range of South Cascade Glacier calculating f at two altitudes gave negligible improvement in estimating winter balance.

In addition to sampling refinements, both temporal and spatial, model terms derived more rigorously from physical principles may lead to better results. When the precipitation flux F was used to estimate precipitation at five stations in the central Cascades of Washington over a 143-day period during the 1996/97 winter, however, the model produced substantially better results than an advanced mesoscale precipitation model (Hayes et al. 2002, Table 6).

4. Upper-air climatology

Regional variation of the mean 1960–99 wind and temperature at 850 mb is shown in Fig. 3 for January and Fig. 4 for October. Distribution of mean October–May 850-mb wind direction varies appreciably over the region (Fig. 5). In the west, near Wolverine, it is predominantly from the southeast, near the major ice concentrations in the vicinity of Yakutat predominantly from the south-southeast, and near the glaciers to the south predominantly from the southwest. In all three locations, winds in the predominant direction are strongest and most humid, as well as being from the ocean toward the glaciers.

The 850-mb wind speed has a pronounced winter maximum throughout the region (Fig. 6). In the northern part RH is nearly uniform seasonally but in the southern part has strong summer minimum, corresponding to the weaker meridional component there in summer. The variations of wind speed and RH combine to produce winter maximum of precipitation flux F as well as of snow flux f.

Negative correlation between winter mass balance of the Alaska glaciers and the ones to the south is also supported by the winter precipitation records at Yakutat and at Forks, which is shown month by month in Fig. 7. The correlation between F at 60°N, 140°W near Yakutat using direction $\phi' = 208°$ and at 47.5°N, 125°W using direction $\phi' = 271°$ follows the same pattern. By contrast, the 850-mb temperature at those two grid points are positively correlated in winter and uncorrelated in summer.

In the absence of mass balance time series for the large glaciers, the precipitation record at nearby Yakutat (Fig. 1) provides an indication of variations in the accumulation from year to year at the large glaciers. The ~90 000 km^2 of glacier area in Alaska is very sparsely sampled by traditional mass balance measurements. Wolverine is well to the west of the major concentration of large glaciers, and Gulkana is well to the north of it. Bering, Hubbard, and Malaspina are tidewater glaciers each greater than 2000 km^2 in area. In the absence of mass balance measurements in this region, variations over time in conditions at 850 mb and at Yakutat can give an indirect indication of how mass balance may be varying on this large mass of ice.

5. Trends

Increasingly negative mass balance since the mid-1980s (Fig. 2) has been noted by Hodge et al. (1998)

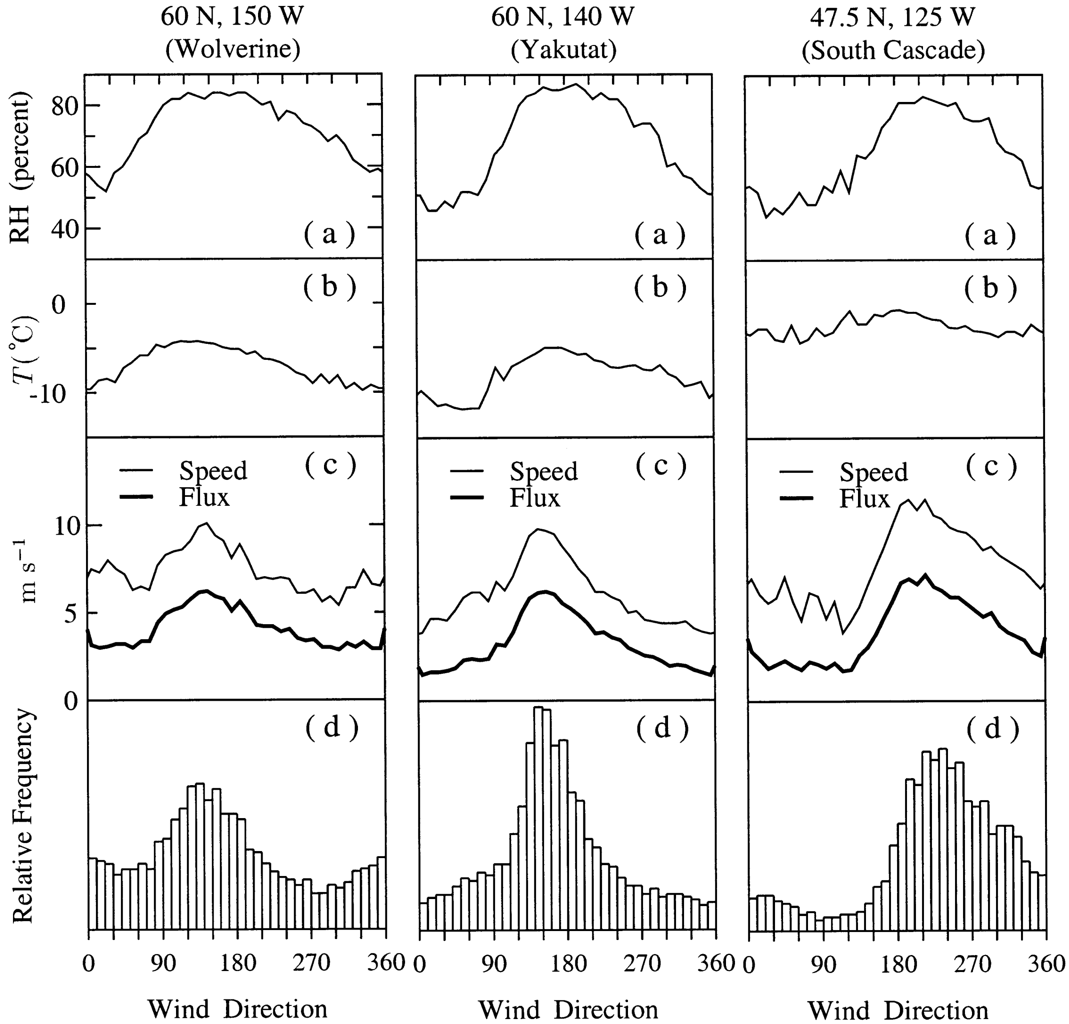

FIG. 5. Mean Oct–May 850-mb values over 1966–99 as a function of wind direction: (a) relative humidity, (b) temperature (°C), (c) wind speed and snow flux *f*, and (d) frequency distribution of wind direction. The flux is RH times the wind speed when $T < +2°C$.

and by Meier and Dyurgerov (2002). Summer balance b_s became increasingly negative since then at all four glaciers considered here. The downward discontinuity in winter balance b_w at Place and South Cascade occurred between 1976 and 1977, at which time Wolverine had an upward discontinuity and Gulkana none.

Discontinuities in glacier mass balances coincide with discontinuities in 850-mb temperature, T_{850}. McCabe and Fountain (1995) noted discontinuity in the mean winter 700-mb heights over western North America in the mid-1970s. A 1976–77 increase $\geq +1°C$ of mean October–May T_{850} occurred over the entire region (Fig. 8). A weaker 1988–89 increase, $\sim +0.8°C$ in mean June–September T_{850}, occurred over a less extensive area (Fig. 9). Variation in T_{850} in the vicinity of the large glaciers (60°N, 140°W) illustrates the 1988–89 summer increase and the 1976–77 winter increase (Fig. 10). Variations at 47.5°N, 125°W show comparable increases in T_{850} but a slightly earlier (1984–85) increase in summer temperature. Winter warming mainly shifts some precipitation from snow to rain, and summer warming mainly increases ablation.

The discontinuity in a time series is defined here to be the shift in the two-stage piecewise-constant function best fitting the series. The time of the discontinuity is determined empirically, and the best-fitting constant in a stage is the mean of the values in that stage. The time is identified by the last year of the first stage and the first year of the second stage, so 1976–77 indicates that the first stage ended in 1976 and the second began in 1977. The difference between the two means is defined to be the magnitude of the discontinuity. For all time series in Figs. 2 and 10, the piecewise-constant function fits the series better than a single linear function fit to the series.

Precipitation records suggest a shift of spatial pattern rather than a change in the total amount over the region. Stafford et al. (2000) found an average increase of about

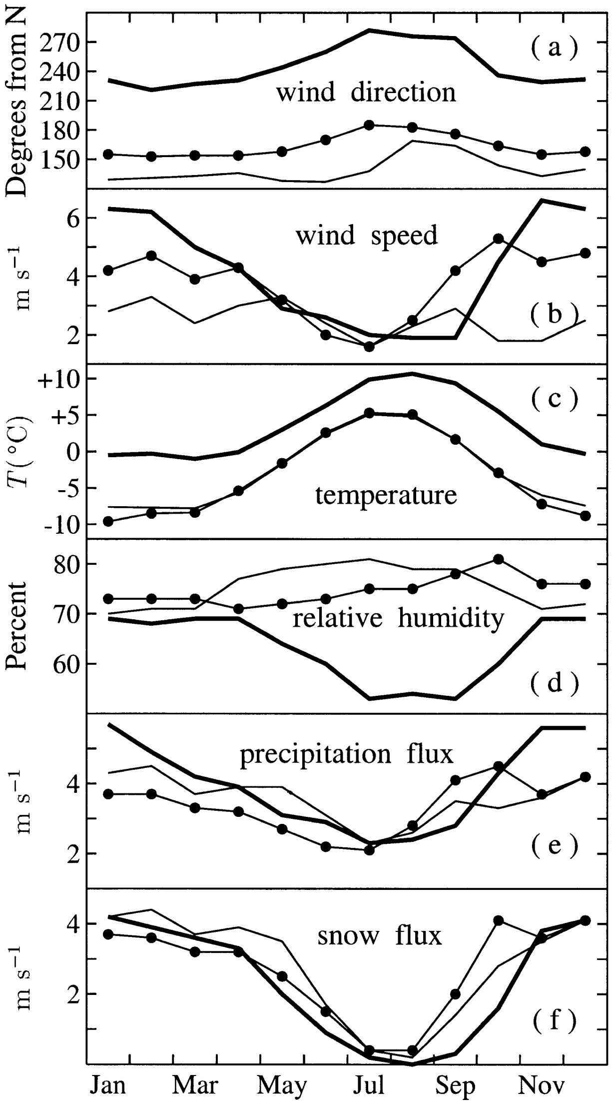

FIG. 6. Seasonal variation of mean 850-mb conditions over 1960–99. The plain light curve is grid point 60°N, 150°W near Wolverine, the dotted light curve is grid point 60°N, 140°W near Yakutat, and the heavy curve is 47.5°N, 125°W near the southern glaciers. Critical azimuth directions ϕ' for the precipitation flux F are, respectively, 122°, 208°, and 271°. Snow flux f is the part of the precipitation flux F when $T_{850} < +2$°C.

10% in southern Alaska over 1949–98. Rasmussen and Conway (2001) found a 1976–77 decrease that averaged about 6% over several stations in western Washington. Mean October–May precipitation at Forks was nearly unchanged, averaging 2.80 m over 1960–76 and 2.70 m over 1977–99, whereas at Yakutat it increased substantially from 2.29 m over 1966–76 to 2.92 m over 1977–98.

There is a pronounced 1976–77 shift in the winter precipitation flux F (Table 5) in both the north and south. Increase at 60°N, 140°W is consistent with the increase in Yakutat precipitation as is the decrease at 47.5°N, 125°W with decrease of precipitation in the south. The

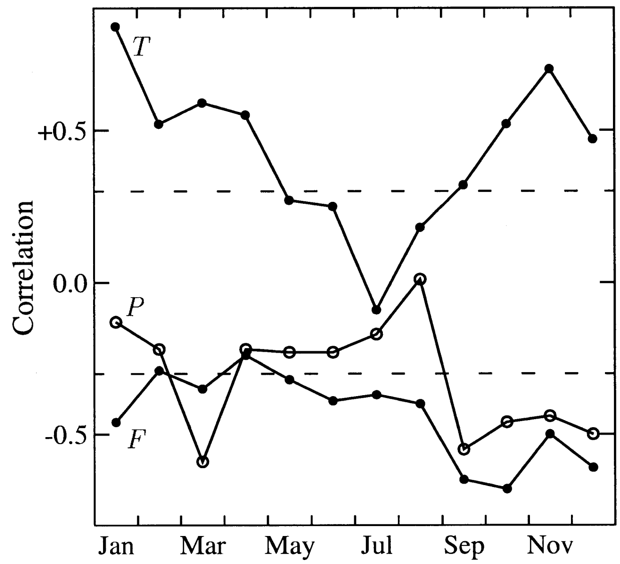

FIG. 7. Monthly variation of correlation of 850-mb temperature (T) and precipitation flux (F) between NCEP–NCAR reanalysis grid points at 47.5°N, 125°W in direction 271°, which is optimum critical direction for estimating South Cascade accumulation, and 60°N, 140°W in direction 208°, which is optimum for estimating Yakutat precipitation. Also shown (P) is correlation between Yakutat and Forks precipitation. All correlations are over 1966–99; those with $|r| \geq 0.30$ (outside the dashed lines) are significant at the 95% level.

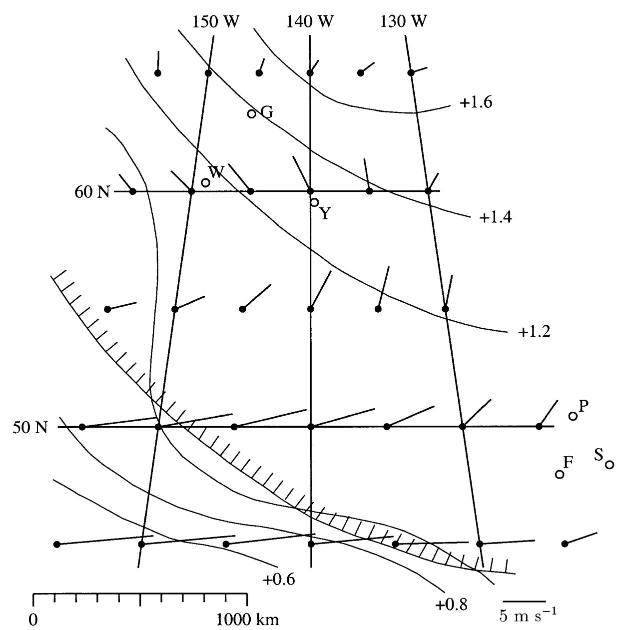

FIG. 8. Increase (°C) of Oct–May 850-mb temperature between 1960–76 mean and 1977–99 mean. At grid points on the ticked side of the ticked contour, the best-fitting two-stage piecewise-constant fit to the 1960–99 series had discontinuity (increase) between 1976 and 1977. Wind vectors for Apr.

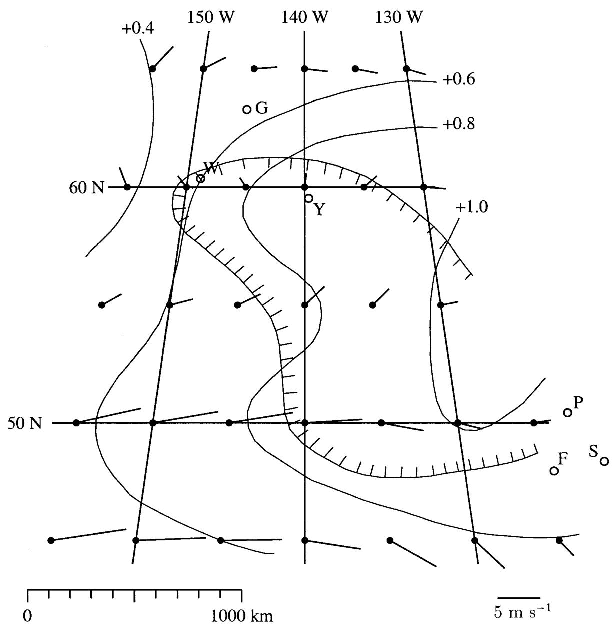

FIG. 9. Increase (°C) of Jun–Sep 850-mb temperature between 1960–88 mean and 1989–99 mean. At grid points on the ticked side of the ticked contour, the best-fitting two-stage piecewise-constant fit to the 1960–99 series had discontinuity (increase) between 1988 and 1989. Wind vectors for Jul.

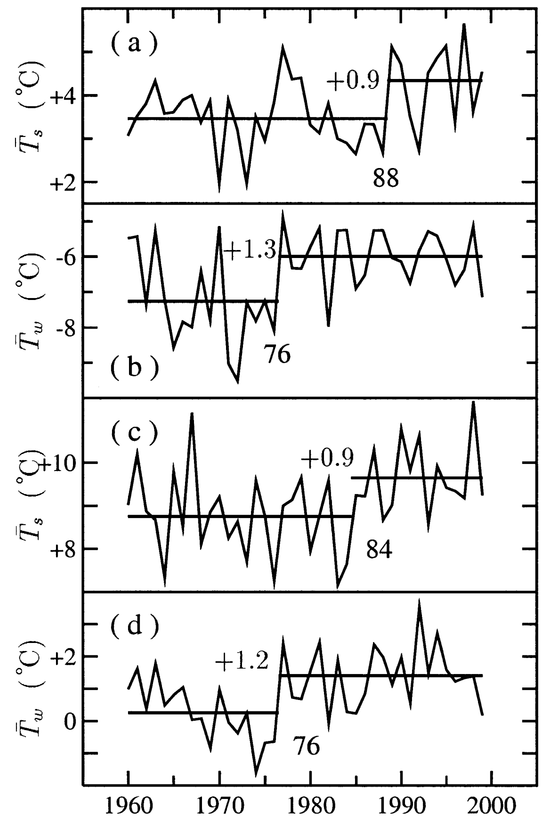

FIG. 10. Variations of mean seasonal 850-mb temperatures. (a) Jun–Sep at 60°N, 140°W (near Yakutat); (b) Oct–May at 60°N, 140°W; (c) Jun–Sep at 47.5°N, 125°W (near Forks); (d) Oct–May at 47.5°N, 125°W. The unsigned number indicates the last year of the first stage of the best-fitting piecewise-constant function, and the signed number is the difference between the mean values of the two stages.

T increase is similar in both regions but in the north T is further below the critical temperature $+2°C$ so that the snow fraction f/F declined less in the north (about 1%) than in the south (about 5%). In the south the F decrease and the f/F decrease both had the effect of reducing the snow flux f, but in the north the F increase overcame the f/F decrease. The large increase in October–May F and hence in f at 60°N, 150°W is consistent with the jump in Wolverine b_w then.

In addition to long-term changes in precipitation, there are interannual variations. Negative correlation of precipitation between Yakutat and Forks (Fig. 7) is an example. Walters and Meier (1989), McCabe and Fountain (1995), Hodge et al. (1998) have all discussed the negative correlation between the Alaska glaciers and the ones to the south in terms of variations in atmospheric circulation patterns and, thus, of the spatial distribution of precipitation. Position and intensity of the Aleutian low is a key feature of the patterns (Trenberth 1990).

6. Conclusions

Although ocean SST exert a profound influence on the atmosphere and ultimately on a glacier, upper-air conditions in its vicinity have a more direct and immediate effect. The temporal variability of the upper-air conditions matches that of the mass balance processes, accumulation and ablation, better than does the seasonal average of SST. Because of nonlinearities in the relations between meteorological conditions and the two processes, long-term averages of large-scale atmospheric or ocean conditions do not correlate as well with long-term totals of accumulation or ablation or,

TABLE 5. Mean Oct–May precipitation flux and snow flux, before 1976 and after. Snow flux f is calculated with direction ϕ' at altitude z_1 by Eqs. (3), (4), and precipitation flux F the same way but without the T_1 restriction, both in m s^{-1}. The mean temperature at z_1 when the wind component U in the direction ϕ' is positive [Eq. (4)] is T_f(°C).

Grid point (°N, °W)	ϕ'	z_1	1960–76				1977–99			
			T_f	F	f	f/F	T_f	F	f	f/F
60.0, 150.0	122	1100	−3.4	2.8	2.7	0.94	−2.4	3.4	3.2	0.92
60.0, 140.0	208	1100	−4.0	2.9	2.7	0.94	−3.3	3.2	3.0	0.93
47.5, 125.0	271	1650	−1.9	3.9	3.1	0.79	−1.0	3.4	2.6	0.75

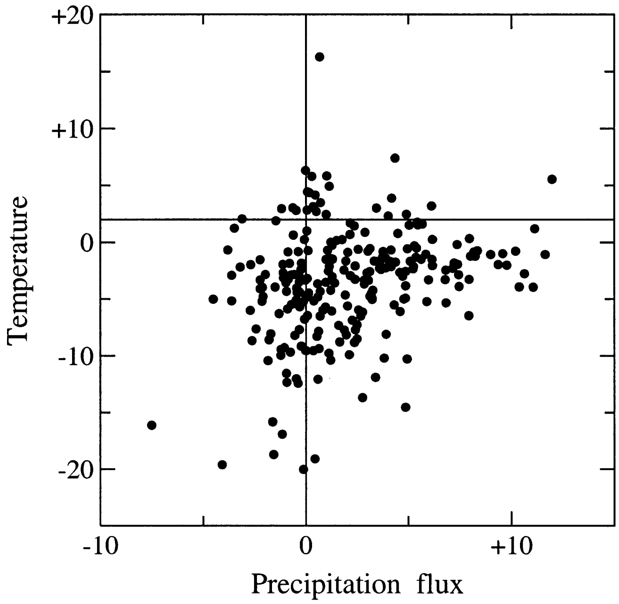

FIG. 11. Precipitation flux F at 850-mb from direction 208° vs 1000-m temperature (°C), Oct 1982 through May 1983 at grid point 60°N, 140°W.

thus, with mass balance components b_w or b_s or their sum b_n (Table 4). On the scale of seasonal averages, however, SST and upper-air temperatures are strongly correlated. Winter warming after 1976 (Fig. 8) and summer warming after 1988 (Fig. 9) coincide with raised SST in the NE Pacific, in winter after 1976 and in summer after 1988 (Fig. 8 of Hare and Mantua 2000).

The need for high temporal resolution of upper-air conditions is illustrated by the day to day covariability of F and temperature. The flux at 60°N, 140°W with critical direction $\phi' = 208°$ is shown in Fig. 11, along with temperature at 1000 m, during October–May of 1982/83 when nearby Yakutat had average precipitation. According to the model presented here, only occurrences in the lower right-hand quadrant, with $F > 0$ and $T \leq +2°$C, contribute to accumulation.

Principal climatological variables pertinent to mass balance processes are winter precipitation, winter temperature, and summer temperature. The first two control mainly accumulation, the third mainly ablation. Over the past 40 years, temperature has undergone marked step increases, 1976–77 in winter and 1988–89 in summer, coherently throughout the region. Changes in precipitation, however, are more complicated. The apparent long-term shift of precipitation from the southern to northern part of the region is accompanied by strong interannual variation of the distribution of precipitation within the region. The negative jump in b_w at Place and South Cascade (Fig. 2) is fostered by both the increase in winter temperature and the decrease in precipitation, both since the mid-1970s. At Wolverine and Gulkana, by contrast, the increase in winter temperature is counteracted by the increase in precipitation. The marked thinning of glaciers in southern Alaska (Arendt et al. 2002), therefore, is probably the result of summer warming.

Determining numerical values for the regression coefficients in the models as well as the critical direction ϕ' and altitudes z_1 and z_2 [Eqs. (2)–(5)] requires a mass balance record. In the absence of a record, rough estimates (ϕ' in the onshore direction, z_1 low on the glacier, and z_2 near the middle of it) permit forming time series of the snow fluxes $\overline{f}_w$, $\overline{f}_s$ and temperature $\overline{T}_2$ from the meteorological database. Relative changes in the fluxes and temperature will give a qualitative indication of relative changes in mass balance components.

Acknowledgments. This work was funded from U. S. National Science Foundation Grant OPP-0240861 and NASA Grant 1215388. Substantial comments by Andrew Fountain led to marked improvement in the clarity of presentation. We thank E. Recker for extracting reanalysis data from NCAR and R. Ludwin for supplying coastline coordinates.

REFERENCES

Angell, J. K., 1988: Variations and trends in tropospheric and stratospheric global temperatures, 1958–87. *J. Climate,* **1,** 1296–1313.

Arendt, A. A., K. A. Echelmeyer, W. D. Harrison, C. S. Lingle, and V. B. Valentine, 2002: Rapid wastage of Alaska glaciers and their contribution to rising sea level. *Science,* **297,** 382–386.

Beamish, R. J., C. E. Neville, and A. J. Cass, 1997: Production of Fraser River sockeye salmon (*Oncorhynchus nerka*) in relation to decadal-scale changes in the climate and the ocean. *Can. J. Fish. Aquat. Sci.,* **54,** 543–554.

Bitz, C. M., and D. S. Battisti, 1999: Interannual to decadal variability in climate and the glacier mass balance in Washington, western Canada, and Alaska. *J. Climate,* **12,** 3181–3196.

Dyurgerov, M. B., 2002: Glacier mass balance and regime: Data of measurements and analysis. Institute of Arctic and Alpine Research, University of Colorado, Occasional Paper 55, 266 pp.

Hare, S. R., and N. J. Mantua, 2000: Empirical evidence for North Pacific regime shifts in 1977 and 1989. *Progress in Oceanography,* Vol. 47, Pergamon, 103–145.

Hayes, P. S., L. A. Rasmussen, and H. Conway, 2002: Estimating precipitation in the central Cascades of Washington. *J. Hydrometeor.,* **3,** 335–346.

Hodge, S. M., D. C. Trabant, R. M. Krimmel, T. A. Heinrichs, R. S. March, and E. G. Josberger, 1998: Climate variations and changes in mass of three glaciers in western North America. *J. Climate,* **11,** 2161–2179.

Kalnay, E., and Coauthors, 1996: The NCEP/NCAR 40-Year Reanalysis Project. *Bull. Amer. Meteor. Soc.,* **77,** 437–471.

Kistler, R., and Coauthors, 2001: The NCEP–NCAR 50-year reanalysis: Monthly means CD-ROM and documentation. *Bull. Amer. Meteor. Soc.,* **82,** 247–267.

Krimmel, R. M., 2000: Water, ice, and meteorological measurements at South Cascade Glacier, Washington, 1986–1991 balance years. U.S. Geological Survey Water-Resources Investigations Rep. 00-4006, 77 pp.

——, 2002: Water, ice, and meteorological measurements at South Cascade Glacier, Washington, 2000–01 balance years. U.S. Geological Survey Water-Resources Investigations Rep. 02-4165, 63 pp.

Mayo, L. R., M. F. Meier, and W. V. Tangborn, 1972: A system to combine stratigraphic and annual mass-balance systems. *J. Glaciol.,* **11,** 3–14.

McCabe, G. J., and A. G. Fountain, 1995: Relations between atmospheric circulation and mass balance of South Cascade Glacier, Washington, U.S.A. *Arct. Alp. Res.,* **27,** 226–233.

McFarlane, G. A., J. R. King, and R. J. Beamish, 2000: Have there been recent changes in climate? *Progress in Oceanography*, Vol. 47, 147–169.

Meier, M. F., and M. B. Dyurgerov, 2002: How Alaska affects the world. *Science,* **297,** 350–351.

——, W. V. Tangborn, L. R. Mayo, and A. Post, 1971: Combined ice and water balances of Gulkana and Wolverine Glaciers, Alaska, and South Cascade Glacier, Washington, 1965 and 1966 hydrologic years. U.S. Geological Survey Prof. Paper 715-A, 23 pp.

Moore, R. D., and M. N. Demuth, 2001: Mass balance and streamflow variability at Place Glacier, Canada, in relation to recent climate fluctuations. *Hydrol. Processes,* **15,** 3474–3486.

Oerlemans, J., and N. C. Hoogendoorn, 1989: Mass balance gradients and climatic change. *J. Glaciol.,* **35,** 399–405.

Pandey, G. R., D. R. Cayan, and K. P. Georgakakos, 1999: Precipitation structure in the Sierra Nevada of California during winter. *J. Geophys. Res.,* **104,** 12 019–12 030.

Rasmussen, L. A., and H. Conway, 2001: Estimating South Cascade Glacier (Washington, U.S.A.) mass balance from a distant radiosonde and comparison with Blue Glacier. *J. Glaciol.,* **47,** 579–588.

——, and ——, 2003: Using NCEP–NCAR Reanalysis data to estimate South Cascade Glacier (U.S.A.) summer balance. *J. Glaciol.,* **49,** 456–462.

——, ——, and P. S. Hayes, 2000: The accumulation regime of Blue Glacier, U.S.A., 1914–96. *J. Glaciol.,* **46,** 326–334.

——, ——, and ——, 2001: Estimating Olympic Peninsula precipitation from upper-air wind and humidity. *J. Geophys. Res.,* **106,** 1493–1501.

Stafford, J. M., G. Wendler, and J. Curtis, 2000: Temperature and precipitation of Alaska: 50 year trend analysis. *Theor. Appl. Climatol.,* **67,** 33–44.

Trenberth, K. E., 1990: Recent observed interdecadal climate changes in the Northern Hemisphere. *Bull. Amer. Meteor. Soc.,* **71,** 988–993.

——, and J. W. Hurrell, 1994: Decadal atmosphere–ocean variations in the Pacific. *Climate Dyn.,* **9,** 303–319.

U.S. Navy, 1966: *Selected Level Heights, Temperatures and Dew Points for the Northern Hemisphere.* NAVAIR Rep. 50-1C-52, U.S. Navy, Chief of Naval Operations, 429 pp.

Walters, R. A., and M. F. Meier, 1989: Variability of glacier mass balance in western North America. *Aspects of Climate Variability in the Pacific and Western Americas, Geophys. Monogr.,* No. 55, Amer. Geophys. Union, 365–374.